APL Photonics

LETTER | NOVEMBER 01 2024

Tunable kHz distributed feedback fiber laser fabricated in 3D-printed glass

Pawel Maniewski ; Alex I. Flint ; Rex H. S. Bannerman; Timothy Lee ; Martynas Beresna

APL Photonics 9, 111301 (2024)
https://doi.org/10.1063/5.0232419

Tunable kHz distributed feedback fiber laser fabricated in 3D-printed glass

Cite as: APL Photon. 9, 111301 (2024); doi: 10.1063/5.0232419
Submitted: 7 August 2024 • Accepted: 14 October 2024 •
Published Online: 1 November 2024

Pawel Maniewski,[1,2,a] Alex I. Flint,[2] Rex H. S. Bannerman,[2] Timothy Lee,[2] and Martynas Beresna[2]

AFFILIATIONS

[1] Department of Applied Physics, KTH Royal Institute of Technology, Stockholm, Sweden
[2] Optoelectronic Research Centre, University of Southampton, Southampton, United Kingdom

[a] Author to whom correspondence should be addressed: pawelma@kth.se

ABSTRACT

For short sections of fiber tailored to a specific application, fast laser-based manufacturing techniques can be considered as an attractive alternative to the often-cumbersome traditional manufacturing routes. With the use of high-power lasers, localized hot zones that are necessary for glass making can be obtained rapidly. For instance, laser-powder-deposition enables rapid fabrication of short, high gain fibers used in, e.g., distributed feedback fiber lasers (DFFLs). DFFLs offer sought after performance suitable for a broad range of applications in modern photonics, i.e., superior stability and narrower, single-frequency linewidth compared to conventional fiber lasers. Tunable, narrow laser sources with output in an eye-safe spectrum are desired for sensing, signal multiplexing, LIDAR systems, quantum applications, etc. In this work, we present DFFL obtained using laser-powder-deposition made Er-doped silica fiber. Milliwatt level, narrow line lasing (<704 kHz, equipment limited) was obtained using a phase-shifted grating written in 16 mm long fiber. The backward slope efficiency was as high as 24% when pumping at 976 nm. The results presented in this work showcase new possibilities in fiber fabrication that were unlocked through laser-assisted additive manufacturing. This fiber laser sets the stage for the future of rapid fabrication of advanced fiber devices through unconventional manufacturing routes.

I. INTRODUCTION

Photonics devices based on silica fibers are highly regarded for their low transmission loss, robustness, and easy integration with the existing infrastructure. The physicochemical properties of silica glass make these fibers suitable to work in, e.g., harsh environments.[1–3] These properties can be modified by doping the glass network with other elements. For instance, by doping silica with Ge^{4+} or Al^{3+}, its refractive index can be increased. A doped core combined with pure silica cladding is often used to obtain the typical step-index profile of the optical fiber. Furthermore, doping the silica fiber core with rare-earth (RE) enables optical gain in a relatively broad spectral range.[4] For narrow linewidth emission, selective feedback can be used, such as the reflection from a fiber Bragg grating (FBG). To obtain the grating, UV lasers or pulsed high peak power, i.e., femtosecond lasers (femtosecond laser writing—FLW), are typically used.[5–7] In the case of UV-based writing, photosensitivity of the fiber is required. The latter can be obtained through doping with germanium (during fiber fabrication)[8] or hydrogen loading (post-processing).[9] In the case of FLW, photosensitivity is not required, as modification is created using nonlinear absorption responsible for triggering initial seed electrons.[10] Furthermore, FLW obtained type II gratings, i.e., creating periodic damage in the fiber, can be preferred for some applications due to their long-term stability and robustness.

The distributed feedback fiber laser (DFFL) is a special type of fiber laser that utilizes a periodic modulation of refractive index within the active fiber to provide both gain and feedback for lasing. Typically, to obtain the feedback, a phase-shifted Bragg grating is written directly into the core of an active fiber and, thus, acts as a distributed reflector.[11–13] The phase-shift introduces a localized resonance and only allows operation in a single longitudinal mode.[14] Such grating structures typically produce a stable, narrow linewidth output desirable in many applications. For instance, in telecoms, narrow linewidth sources within C-band (1530–1565 nm) enhance the performance, reliability, and capacity of telecommuni-

cation systems by enabling precise modulation and reducing signal crosstalk.[15–17] Gain in the C-band is often obtained through Er-doping and typical pumping schemes at 980 or 1480 nm.[14]

Generally, to obtain a high gain per unit length, a high doping concentration is desired. However, in the standard Er-doped fiber fabrication processes, e.g., using modified chemical vapor deposition, the dopant concentration is often limited by the Er-ion clustering, leading to increasingly efficient cooperative upconversion processes. Both cause the so-called concentration quenching of the optical gain.[18,19] Alternatively, laser powder deposition (LPD) can be used to obtain silica-based glass rods with desired doping. The high deposition rate of >1 mm^3/s enables the complete fabrication of glass rods in under a minute. The printed glass rods are then used as components for fiber manufacturing, similar to the rod-in-tube technique. In LPD, a mid-IR CO_2 laser is used to locally melt and sinter oxide powders delivered into the beam via off-axis jets.[20] Leveraging this additive manufacturing (AM) approach enables working with smaller production batch sizes, decreasing the length of each production cycle to expedite material optimization.[4] Furthermore, some of the desired doping schedules can be achieved through powder mixing rather than the more cumbersome, traditionally used, solution doping. In RE-doped specialty fiber manufacturing, LPD enables high doping concentrations with minimal clustering.[21] Low clustering combined with high doping allows the utilization of shorter fibers without sacrificing the gain. Consequently, short fibers mitigate undesirable nonlinear effects in the cavity, e.g., stimulated Brillouin scattering or stimulated Raman scattering.[22,23] In this work, we showcase a tunable DFFL that was enabled by the combination of short, LPD-made Er-doped fiber and direct laser writing. The results presented in this work showcase new possibilities in fiber fabrication that were unlocked through laser-assisted AM. This narrow line fiber laser with precise tunability with temperature sets the stage for the future of rapid fabrication of advanced fiber devices.

II. DFFL FABRICATION

To obtain the laser, first, a cylindrical rod was produced through laser powder deposition. Here, a dry nanopowder mixture of SiO_2, Al_2O_3, and Er_2O_3 (all: US Research Nanomaterials Inc.; >99.9% purity powders were used in our experiments) was prepared using a custom-made stainless-steel ball-mill. The ratio of powders was 94:5.3:0.7 wt %, respectively. Subsequently, a mid-IR CO_2 laser (λ = 10.6 μm) was used to sinter a nanopowder mixture as described in the procedure of rapid fabrication of silica specialty fibers.[24] To obtain the rod, a substrate plate (1 mm thick quartz) was mounted on a two-axis translation stage (x–y). The laser beam (P = 47 W) was launched normally and focused using a ZnSe lens (f = 40 mm) onto a substrate, creating a 1 mm wide melt-pool in the substrate. In our experiments, the rod was obtained by vertical translation (z) of the lens (v = 1 mm/s) while feeding the powders.[25] The rod was then removed from the substrate and sleeved in a quartz tube to form a preform with an outside diameter of 6 mm, and then it was drawn into a fiber that had a ~125 μm outer diameter. Approximately 50 m of fiber has been drawn. The fiber had an effective refractive index of the core mode of approximately n ≈ 1.4484 (at λ = 1550 nm), while the transmission loss of the fiber at λ_p = 976 nm was ~14.8 dB/m. The loss was estimated using 12 consecutive cutbacks, ~2 cm long each. The high loss was in line with our expectations, as this wavelength corresponds to one of the absorption bands of Er^{3+}. The background loss was estimated to be less than 1 dB/m (measured at λ = 1342 nm); however, a more accurate approximation was limited by the short length of the drawn fiber. The drawn fiber was cleaved using a standard cleaver equipped with a diamond blade and then spliced to a commercial single mode fiber.

A third order grating was written to ensure high contrast of the grating pitch and uniformity of the grating. To obtain the grating, a plane-by-plane FLW approach was used,[26] i.e., the DFFL structure was inscribed by translation of the fiber with respect to the stationary beam across and along its axis as sketched in Fig. 1. The DFFL structure can be simply thought of as two identical gratings separated by a single π-phase shift. A frequency doubled (515 nm) femtosecond Yb:KGW laser system (Pharos SP, Light Conversion Ltd.) operating at 200 kHz was used for grating the inscription. First, the fiber was fixed onto a quartz plate and immersed in silica index-matching oil [Cargille, n = 1.4587 (λ = 589.3 nm)]. The laser beam (M^2 < 1.2) was focused using an oil immersion microscope objective with a variable numerical aperture (Olympus Plan N 50 × /0.5–0.9) in the axial plane of the fiber core. Specific writing parameters were experimentally optimized to obtain low loss and high contrast of the grating. For our application type I, grating was desired. In Table I, the writing parameters used for the DFFL are shown. During writing, the core was irradiated only during the scans across the core (100 μm/s), while each consecutive plane was offset using translation at low speed (50 μm/s) to avoid errors produced by acceleration and

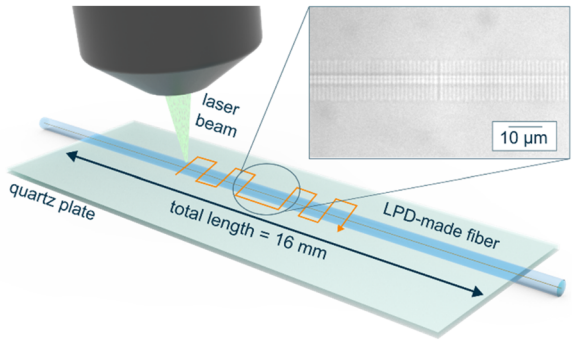

FIG. 1. Schematic of fs-laser writing of DFFL. The inset shows a micrograph of the fiber core with fabricated grating (contrast increased for clarity).

TABLE I. Parameters used for DFFL writing.

P_{avg} (incident on the fiber)	6.2 mW
Wavelength	515 nm
Rep. rate	200 kHz
Pulse energy	30 nJ
Objective NA	0.5
M^2	<1.2
Speed x (along the fiber)	50 μm/s
Speed y (across the fiber)	100 μm/s

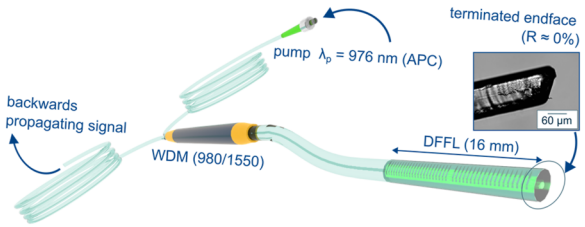

FIG. 2. Schematic of DFFL experimental setup.

deceleration of the stage. In other words, the slow scans allowed precise control of the position of each plane of the grating. In the FLW system, a dichroic mirror was placed above the focusing objective, and it was used to monitor the writing process in real-time using a CMOS camera. This monitoring system also allows for the positioning of the fiber with respect to the laser focal point with sub-micron precision.

For the writing, the 16 mm long LPD-obtained fiber was mounted onto a quartz plate under slight tension. The quartz plate was mounted via a custom made sample holder onto Aerotech ANT130-160-XY stages. To compensate for a slight misalignment of the fiber, the start and end points of the grating were mapped in three dimensions prior to writing. This step also ensured optimal distribution of the grating throughout the whole length of the active fiber. The total length of the used gain fiber (and the grating) was 16 mm with a centrally located phase-shift. To monitor the grating inscription, a pump diode laser (λ_p) was coupled into the fiber via a wavelength-division-multiplexer (WDM), and an optical spectrum analyzer (OSA, Yokogawa AQ6370) was used to monitor the signal in reflection. Such an arrangement enabled observation of how the inscribed grating was affecting the amplified spontaneous emission signal and confirmed lasing after the DFFL structure was completed.

III. PERFORMANCE EVALUATION

To assess the performance of the fiber and the cavity, a simple test setup was used in order to reduce the impact of unrelated factors. A schematic of the DFFL experimental setup is shown in Fig. 2. The forward output face was terminated by mechanical crushing in order to restrain any back reflections (see inset in Fig. 2). Using a laser diode (λ_p = 976 nm, BL976, Thorlabs Inc.) as a pump, a lasing threshold of 1.29 mW was obtained. An upper limit of the backward output linewidth was determined by heterodyne measurement. The backward propagating DFFL output was combined with a local oscillator (Agilent 81600B) using a 50:50 beam splitter. The beat note between the two lasers was then measured. A fast photodiode (PDA8GS Thorlabs Inc.) and an electrical spectrum analyzer (AVANTEST R3273) with a scanning time of 30 ms were used. The 3 dB linewidth was found to be 704 kHz, as shown in Fig. 3(a). The

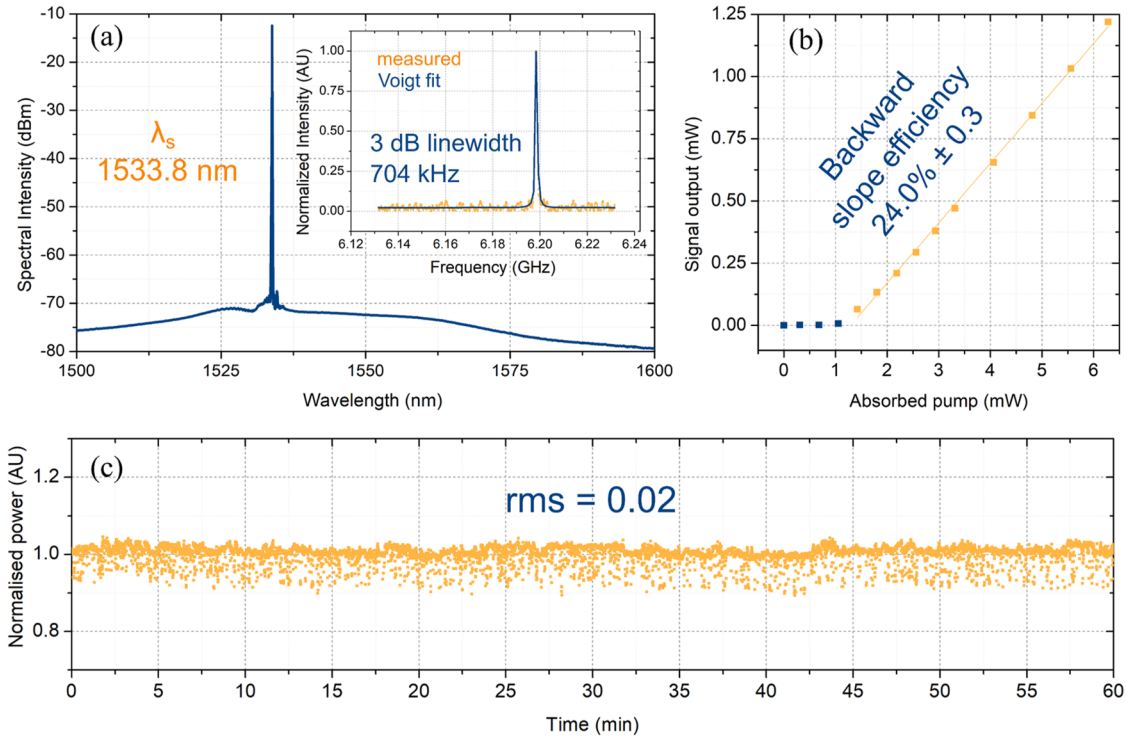

FIG. 3. DFFL output spectrum obtained readily post-FLW (a) and a normalized heterodyne beat note with a local oscillator (inset) and its backward slope efficiency (b) against the absorbed pump. Normalized to average power stability (c) at maximum output.

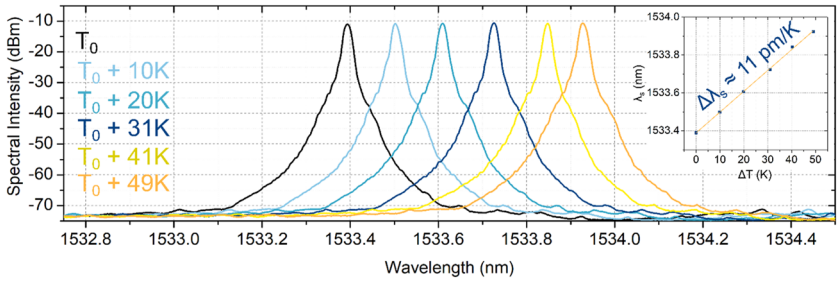

FIG. 4. Spectral intensity of the DFFL's output at different temperatures (T_0—room temperature). The inset shows the shift of the laser peak, which corresponds to 11 pm/K.

beat note in such a measurement is larger than the linewidth of the lasers used,[27,28] and therefore, the true linewidth is expected to be narrower.

Backward slope efficiency of up to 24% was measured against the absorbed pump (see Fig. 3). It is noteworthy that due to the simple symmetric-grating design utilized in this study, DFFL was lasing in both directions. Our focus on this straightforward design allows for a clear demonstration of the lasing performance, while more complex cavity designs are well-documented in the literature and can be utilized in our future work. Power stability was measured, and a variation of up to 2% was found when running at maximum power for over 1 h. A sampling rate of 2 Hz was used.

The thermal shift of the output was investigated at elevated temperatures, as shown in Fig. 4. To assess the shift of the laser, it was mounted onto a silicone heating mat and placed in an insulated box. The output was monitored using the OSA. The temperature offset was measured with a thermocouple placed in close proximity to the fiber. A shift of ~11 pm/K was observed in temperatures up to 345 K, and it is in line with typically measured shifts and can be linked to composition dependent thermal expansion and the thermo-optic effect in silica.[29]

IV. SUMMARY

In summary, in this work, we demonstrated, to the best of our knowledge, the first narrow linewidth fiber laser that was based on short, active fiber obtained through additive manufacturing. Here, selective, distributed feedback was obtained using a femtosecond laser direct writing method. This approach significantly reduces fabrication time while enhancing device performance. However, challenges related to powder purity and maintaining high quality of core/cladding interface should be carefully addressed when combining LPD with the rod-in-tube method. Demonstrated here is eye-safe, milliwatt output, showing high stability and high efficiency. The high efficiency of up to 24% of the laser, only measured backward, is one of the highest reported for this type of material, doping, and pump scheme.[11,12,30] Further improvements that include, e.g., co-doping with Yb^{3+} to improve pump absorption[14,15,31] or more complex DFFL cavity structures can be included in our future work. Nonetheless, the results presented in this paper underline the high quality of the LPD-obtained fiber and its suitability for DFFLs. The results represent a significant advancement in unconventional fiber laser manufacturing and, thus, rapid prototyping of future fiber sources. It also showcases new possibilities for the swift production of tailored, high-performance devices that can be used in various high-tech fields.

SUPPLEMENTARY MATERIAL

See the supplementary material for complete datasets for Figs. 3 and 4.

ACKNOWLEDGMENTS

The authors would like to thank Peter Horak for the insightful conversations and feedback on this work. We would also like to acknowledge funding from the Swedish Research Council (No. 2022–06180), Stiftelsen Tornspiran (No. 894) and the Engineering and Physical Sciences Research Council (Grant No. EP/R513325/1).

AUTHOR DECLARATIONS

Conflict of Interest

The authors have no conflicts to disclose.

Author Contributions

P.M. designed and fabricated the fiber and conceptualized the study; A.I.F., R.H.S.B., and P.M. characterized the laser; R.H.S.B. investigated UV sensitivity of the fiber; M.B., T.L., and P.M. investigated laser writing and inscribed the grating. All authors analyzed and reviewed the results and participated in writing the manuscript.

Pawel Maniewski: Conceptualization (lead); Formal analysis (equal); Funding acquisition (lead); Investigation (equal); Methodology (equal); Resources (equal); Supervision (lead); Visualization (lead); Writing – original draft (lead); Writing – review & editing (equal). **Alex I. Flint**: Data curation (equal); Formal analysis (equal); Investigation (equal); Methodology (equal); Writing – review & editing (equal). **Rex H. S. Bannerman**: Formal analysis (equal); Investigation (equal); Writing – review & editing (equal). **Timothy Lee**: Investigation (equal); Methodology (equal); Writing – review & editing (equal). **Martynas Beresna**: Funding acquisition (equal); Investigation (equal); Methodology (equal); Resources

(equal); Writing – original draft (equal); Writing – review & editing (equal).

DATA AVAILABILITY

The data that support the findings of this study are available within the article and its supplementary material.

REFERENCES

[1] Y. Wang, M. Cavillon, J. Ballato, T. Hawkins, T. Elsmann, M. Rothhardt, R. Desmarchelier, G. Laffont, B. Poumellec, and M. Lancry, "3D laser engineering of molten core optical fibers: Toward a new generation of harsh environment sensing devices," Adv. Opt. Mater. **10**, 2200379 (2022).

[2] Y. Deng and J. Jiang, "Optical fiber sensors in extreme temperature and radiation environments: A review," IEEE Sens. J. **22**, 13811–13834 (2022).

[3] R. Min, Z. Liu, L. Pereira, C. Yang, Q. Sui, and C. Marques, "Optical fiber sensing for marine environment and marine structural health monitoring: A review," Opt Laser. Technol. **140**, 107082 (2021).

[4] P. Maniewski, T. J. Wörmann, V. Pasiskevicius, C. Holmes, J. C. Gates, and F. Laurell, "Advances in laser-based manufacturing techniques for specialty optical fiber," J. Am. Ceram. Soc. **107**, 5143–5158 (2024).

[5] D. Grobnic, S. J. Mihailov, J. Ballato, and P. D. Dragic, "Type I and II Bragg gratings made with infrared femtosecond radiation in high and low alumina content aluminosilicate optical fibers," Optica **2**, 313 (2015).

[6] W. J. Reichman, J. W. Chan, C. W. Smelser, S. J. Mihailov, and D. M. Krol, "Spectroscopic characterization of different femtosecond laser modification regimes in fused silica," J. Opt. Soc. Am. B **24**, 1627 (2007).

[7] Y. Wang, S. Wei, M. Cavillon, B. Sapaly, B. Poumellec, G.-D. Peng, J. Canning, and M. Lancry, "Thermal stability of type II modifications inscribed by femtosecond laser in a fiber drawn from a 3D printed preform," Appl. Sci. **11**, 600 (2021).

[8] M. Franczyk, T. Stefaniuk, A. Anuszkiewicz, R. Kasztelanic, D. Pysz, A. Filipkowski, T. Osuch, and R. Buczynski, "Nanostructured active and photosensitive silica glass for fiber lasers with built-in Bragg gratings," Opt. Express **29**, 10659 (2021).

[9] P. J. Lemaire, R. M. Atkins, V. Mizrahi, and W. A. Reed, "High pressure H_2 loading as a technique for achieving ultrahigh UV photosensitivity and thermal sensitivity in GeO_2 doped optical fibres," Electron. Lett. **29**, 1191 (1993).

[10] M. Beresna, M. Gecevičius, and P. G. Kazansky, "Ultrafast laser direct writing and nanostructuring in transparent materials," Adv. Opt. Photonics **6**, 293 (2014).

[11] W. Sun, J. Shi, Y. Yu, and X. Feng, "All-fiber 1.55 μm erbium-doped distributed-feedback laser with single-polarization, single-frequency output by femtosecond laser line-by-line direct-writing," OSA Continuum **4**, 334 (2021).

[12] W. H. Loh and R. I. Laming, "1.55 μm phase-shifted distributed feedback fibre laser," Electron. Lett. **31**, 1440–1442 (1995).

[13] M. I. Skvortsov, A. A. Wolf, A. V. Dostovalov, A. A. Vlasov, V. A. Akulov, and S. A. Babin, "Distributed feedback fiber laser based on a fiber Bragg grating inscribed using the femtosecond point-by-point technique," Laser Phys. Lett. **15**, 035103 (2018).

[14] M. J. F. Digonnet, *Rare-Earth-Doped Fiber Lasers and Amplifiers, Second, Revised* (Marcel Dekker Inc., 2001).

[15] D. Lipatov, O. Egorova, A. Rybaltovsky, A. Abramov, A. Lobanov, A. Umnikov, M. Yashkov, and S. Semjonov, "Highly Er/Yb-Co-doped photosensitive core fiber for the development of single-frequency telecom lasers," Photonics **10**, 796 (2023).

[16] D. A. Davydov, A. A. Rybaltovsky, S. S. Aleshkina, V. V. Velmiskin, M. E. Likhachev, S. M. Popov, D. V. Ryakhovskiy, Y. K. Chamorovskiy, A. A. Umnikov, and D. S. Lipatov, "An ytterbium-doped narrow-bandwidth randomly distributed feedback laser emitting at a wavelength of 976 nm," Photonics **10**, 951 (2023).

[17] E. Ronnekleiv, S. W. Lovseth, and J. T. Kringlebotn, "Er-doped fiber distributed feedback lasers: Properties, applications and design considerations," Proc. SPIE **4943**, (2003).

[18] J. L. Wagener, D. J. DiGiovanni, P. F. Wysocki, M. J. F. Digonnet, and H. J. Shaw, "Effects of concentration and clusters in erbium-doped fiber lasers," Opt. Lett. **18**, 2014 (1993).

[19] W. L. Barnes, P. R. Morkel, L. Reekie, and D. N. Payne, "High-quantum-efficiency Er^{3+} fiber lasers pumped at 980 nm," Opt. Lett. **14**, 1002 (1989).

[20] P. Maniewski, F. Laurell, and M. Fokine, "Laser cladding of transparent fused silica glass using sub-μm powder," Opt. Mater. Express **11**, 3056–3070 (2021).

[21] P. Maniewski, M. Brunzell, L. Barrett, C. Harvey, V. Pasiskevicius, and F. Laurell, "Er-doped silica fiber laser made by powder-based additive manufacturing," Optica **10**, 1280–1286 (2023).

[22] R. G. Smith, "Optical power handling capacity of low loss optical fibers as determined by stimulated Raman and Brillouin scattering," Appl. Opt. **11**, 2489 (1972).

[23] J. O. White, A. Vasilyev, J. P. Cahill, N. Satyan, O. Okusaga, G. Rakuljic, C. E. Mungan, and A. Yariv, "Suppression of stimulated Brillouin scattering in optical fibers using a linearly chirped diode laser," Opt. Express **20**, 15872 (2012).

[24] P. Maniewski, C. M. Harvey, K. Mühlberger, T. Oriekhov, M. Brunzell, F. Laurell, and M. Fokine, "Rapid prototyping of silica optical fibers," Opt. Mater. Express **12**, 2426 (2022).

[25] P. Maniewski, F. Laurell, and M. Fokine, "Quill-free additive manufacturing of fused silica glass," Opt. Mater. Express **12**, 1480–1490 (2022).

[26] K. Zhou, M. Dubov, C. Mou, L. Zhang, V. K. Mezentsev, and I. Bennion, "Line-by-Line fiber Bragg grating made by femtosecond laser," IEEE Photonics Technol. Lett. **22**, 1190–1192 (2010).

[27] S. V. Kashanian, A. Eloy, W. Guerin, M. Lintz, M. Fouché, and R. Kaiser, "Noise spectroscopy with large clouds of cold atoms," Phys. Rev. A **94**, 043622 (2016).

[28] Z. Bai, Z. Zhao, Y. Qi, J. Ding, S. Li, X. Yan, Y. Wang, and Z. Lu, "Narrow-linewidth laser linewidth measurement technology," Front. Phys. **9**, 768165 (2021).

[29] A. D. Kersey, M. A. Davis, H. J. Patrick, M. LeBlanc, K. P. Koo, C. G. Askins, M. A. Putnam, and E. J. Friebele, "Fiber grating sensors," J. Lightwave Technol. **15**, 1442–1463 (1997).

[30] J.-Q. Cheng and S.-C. Ruan, "Erbium-doped photonic crystal fiber distributed feedback loop laser operating at 1550nm," Opt. Laser. Technol. **44**, 177–179 (2012).

[31] J. E. Townsend, W. L. Barnes, K. P. Jedrzejewski, and S. G. Grubb, "Yb^{3+} sensitised Er^{3+} doped silica optical fibre with ultrahigh transfer efficiency and gain," Electron. Lett. **27**, 1958 (1991).